

Original Article

MiR-136-5p is involved in the pathogenesis of LUSC through targeting MTDH: a study based on RT-qPCR, IHC, public database and dual-luciferase reporter assay

Li Gao^{1*}, Tiantian Li^{2*}, Binliang Gan², Xiang Gao², Zucheng Xie¹, Rongquan He², Weijia Mo¹, Xiaojv Chi²

Departments of ¹Pathology, ²Medical Oncology, The First Affiliated Hospital of Guangxi Medical University, 6 Shuangyong Road, Nanning 530021, Guangxi Zhuang Autonomous Region, China. *Equal contributors and co-first authors.

Received October 25, 2017; Accepted July 5, 2018; Epub October 15, 2018; Published October 30, 2018

Abstract: MiRNAs have been implicated to be involved in the carcinogenesis and development of human cancers. This study was designed to investigate the clinic-pathological significance of miR-136-5p in lung squamous cell carcinoma (LUSC) and the underlying molecular mechanism. We analyzed expression of miR-136-5p in LUSC with available data from the cancer genome atlas (TCGA). Real-time quantitative polymerase chain reaction (RT-qPCR) was conducted to further verify the results from TCGA. Then we identified the differential expression level of MTDH in LUSC and non-cancer tissues via immunohistochemistry (IHC) and data mining of public databases. Furthermore, the targeting regulatory relationship between miR-136-5p and MTDH was validated by dual luciferase reporter assay. According to the results, miR-136-5p exhibited lower expression in LUSC tissues than in non-cancer tissues and was significantly associated with TNM stage of LUSC ($P = 0.001$). MTDH presented notable overexpression in LUSC ($P = 0.041$). Statistical analysis for IHC suggested that MTDH was positively correlated with lymph node metastasis ($P = 0.010$) and tumor size ($P = 0.009$). Moreover, results from dual luciferase reporter assay evidenced MTDH as a direct target of miR-136-5p. Bioinformatics analysis revealed that miR-136-5p might be involved in vasculature development, focal adhesion and mitogen-activated protein kinases. In summary, miR-136-5p and MTDH can be treated as a break through point for the improved diagnosis and therapy of LUSC.

Keywords: miR-136-5p, MTDH, lung squamous cell carcinoma, RT-qPCR, IHC, dual-luciferase reporter assay

Introduction

Lung cancer tops the list of causes of cancer-related mortality in both males and females worldwide [1, 2]. Based on histological characteristics, lung cancer is further classified into two subtypes: small cell lung cancer (SCLC) and non-small cell lung cancer (NSCLC). NSCLC, including lung adenocarcinoma (LUAD), lung squamous cell carcinoma (LUSC), and large cell lung carcinoma (LCLC), constitutes approximately 80% of all lung cancer cases [3, 4]. LUSC makes up 30% of all NSCLC cases, resulting in approximately 400,000 deaths each year [5, 6]. Molecular targets featuring lymphoma kinase (ALK) and epidermal growth factor receptor (EGFR) mark the milestones in the treatment and prognosis of LUAD; nevertheless these targets failed to yield satisfying response

in patients with LUSC [7-11]. Hence, identifying effective biomarkers for LUSC patients remains an urgent and challenging task for researchers across the world.

MicroRNAs (miRNAs) have been at the forefront of research hotspots that are changing the landscape of exploration into human diseases since its discovery in 2003 [12]. They are a class of small non-protein coding RNAs with 21-25 nucleotides in length and are capable of binding to the 3'UTR region of the target genes at post-transcriptional level [13-16], thus exerting regulatory functions to control diverse biological functions including cell proliferation, differentiation, and apoptosis [17-19]. In recent years, miR-136-5p has been reported to act as a tumor suppressor in various cancers including lung cancer [20, 21], liver cancer [22], gas-

MiR-136-5p and MTDH in lung squamous cell carcinoma

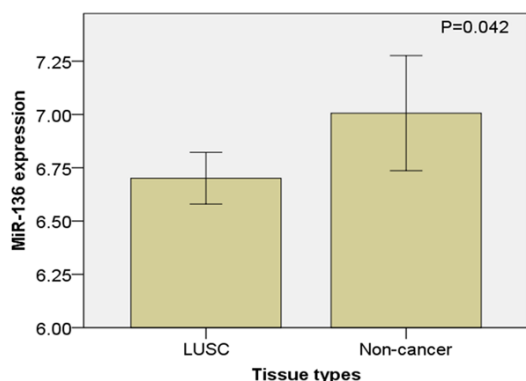


Figure 1. The expression of miR-136 in LUSC from TCGA. Compared with non-cancer tissues (7.006 ± 0.898), miR-136 was significantly down-regulated in LUSC tissues (6.701 ± 1.348) ($P = 0.042$).

tric cancer [23], ovarian cancer [24], breast cancer [25] and glioma [26]. To our knowledge, the role of miR-136-5p in LUSC has not been documented in literature. Hence, the expression and precise underlying mechanism of miR-136-5p in LUSC remains a mystique and requires further elucidation.

MTDH (metadherin), also termed as astrocyte elevated gene-1 (AEG-1) or Lyric (lysine-rich CEACAM1), was found in human fetal astrocytes [27] and has emerged as a pivotal gene involved in the metastasis, chemotherapy sensitivity, and prognosis of various human cancers. In a recent study, MTDH was reported to present overexpression in LUSC tissues and the study further demonstrated that knock-down of MTDH significantly inhibited the proliferation, migration and invasion of LUSC cells [28].

In this study, we aimed to investigate the expression of miR-136-5p and MTDH in LUSC as well as the targeting regulatory relations between miR-136-5p and MTDH in LUSC via multiple approaches including data analysis for the cancer genome atlas (TCGA), real-time quantitative polymerase chain reaction (RT-qPCR), immunohistochemistry (IHC), data mining of public databases and dual luciferase reporter assay and enrichment analysis via bioinformatics tools. We hope that this article may shed some light on the pathogenesis of LUSC and bring new hope for the diagnosis and therapy for LUSC.

Materials and methods

MiR-136-5p expression in LUSC from TCGA

The clinico-pathological information of the precursor of miR-136-5p: miR-136 in LUSC was downloaded from TCGA (<http://cancergenome.nih.gov/>), according to which, the clinico-pathological significance of miR-136 was evaluated in a total of 478 LUSC patients and 45 non-cancer patients.

Patient samples for RT-qPCR

We obtained 23 LUSC tissues and 23 adjacent non-cancer tissues from LUSC patients in The First Affiliated Hospital of Guangxi Medical University during the period of January 2012 to February 2014. Informed consents had been signed by all patients before they participated in this study, and the Ethics Committee of The First Affiliated Hospital of Guangxi Medical University approved this study.

RT-PCR for miRNAs

Extraction and normalization of RNA and RT-qPCR were conducted as the description in previous studies [29-32]. RUN6B and RUN48 served as the internal reference for miR-136-5p. The sequences of miR-136-5p, RUN6B and RUN48 were ACUCCAUUUGUUUGAUGAUGGA, CGCAAGGAUGACACGCAAAUUCGUGAAGCG-UUCCAUAUUUUU and GAUGACCCAGGUAACUCUGAGUGUGUCGUGAUGCCAUCACCGCAGCGC-UCUGACC, respectively. TaqMan[®] MicroRNA Reverse Transcription Kit (4366596, Applied Biosystems, Life Technologies Grand Island, NY 14072 USA) was used to perform the 10 μ l RT reactions. PCR reactions were carried out on Applied Biosystems PCR7900. Each of the experiments was repeated three times, including no-pattern controls. Expression values of miR-136-5p in LUSC and paired non-cancer tissues were calculated using the 2- Δ CT method.

Patient samples for IHC

A total of 175 LUSC tissues and 30 non-cancer tissues processed by formalin-fixation and paraffin-embedding between January 2010 and February 2014 from the First Affiliated Hospital of Guangxi Medical University were collected for IHC of MTDH.

MiR-136-5p and MTDH in lung squamous cell carcinoma

Table 1. Relationships between the expression of miR-136 and clinicopathological parameters in LUSC analyzed by data from the TCGA database

Clinicopathological feature		N	Relevant expression of miR-136 (log2x)		
			Mean ± SD	t	P-value
Tissue	Adjacent non-cancerous lung tissue	45	7.006258 ± 0.8982704	-2.071	0.042*
	LUSC	478	6.700933 ± 1.3482864		
Age (years)	≤ 60	104	6.725499 ± 1.2871274	0.174	0.862
	> 60	367	6.699535 ± 1.3607673		
Gender	Female	124	6.623905 ± 1.3628905	0.739	0.460
	Male	354	6.727915 ± 1.3440295		
Tumor location	Central lung	140	6.863917 ± 1.4289547	-1.393	0.165
	Peripheral lung	91	3.602976 ± 1.3302672		
Stage	Stage I-II	388	6.741586 ± 1.3119826	1.304	0.193
	Stage III-IV	86	6.531803 ± 1.5093940		
T	T1-2	387	6.697083 ± 1.3147723	-0.129	0.898
	T3-4	91	6.6717307 ± 1.4901420		
Pathologic_Stage	Stage I	230	6.735352 ± 1.3481603	F = 2.083 ^a	0.101
	Stage II	158	6.750660 ± 1.2616456		
	Stage III	80	6.513555 ± 1.5454035		
	Stage IV	6	6.775101 ± 0.9589229		
Pathologic_T	T1	106	6.0679143 ± 1.2675678	F = 0.638 ^a	0.591
	T2	281	6.6703851 ± 1.3342953		
	T3	69	6.850572 ± 1.3182463		
	T4	22	6.299341 ± 1.9099961		
N	No	301	6.718984 ± 1.3660542	0.428	0.669
	Yes	171	6.663521 ± 1.3288790		
M	No	390	6.0632008 ± 1.3205963	-0.264	0.792
	Yes	6	6.775101 ± 0.9589229		

Student's unpaired t test was used for comparison between two groups. ^aOne-way analysis of variance (ANOVA) was performed. *P < 0.05 was considered statistically significant.

IHC for MTDH

Immunohistochemistry was performed to detect MTDH expression in all the formalin-fixed and paraffin-embedded LUSC and normal tissues. All the procedures of IHC were implemented strictly following the instructions of the kit. MTDH rabbit polyclonal antibody (Santa Cruz Biotechnology, Inc., Heidelberg, Germany) was used for the immunostaining of MTDH.

Two experienced pathologists blinded to the outcome evaluated the immunohistochemical results of MTDH independently from the aspects of staining intensity and percentage of positive staining. Scores for staining intensity were defined as the following: 0 for negative, 1 for weak, 2 for moderate and 3 for strong. The percentage of positive staining was marked as 1 for < 25%, 2 for 26 to 50%, 3 for 51 to 75%,

and 4 for > 75%. The product of the two items equals to the final immunohistochemical results. A final score ranging from 0 to 2 corresponded to negative immunostaining of MTDH and a final score ranging from 3 to 12 corresponded to positive immunostaining of MTDH.

Validation of MTDH expression in LUSC using public databases

Apart from IHC, the expression of MTDH was verified by some public databases including: HPA, Oncomine and GEPIA. The Human Protein Atlas (HPA) database is a program dedicated to the investigation of proteome in a wide type of normal human tissues and cancer tissues based on RNA-sequencing analysis and immunohistochemistry analysis [33]. Oncomine is a huge repertory that stores abundant gene expression data in diverse human cancers [34,

MiR-136-5p and MTDH in lung squamous cell carcinoma

Table 2. Relationships between the expression of miR-136-5p and clinicopathological parameters in LUSC analyzed by data from RT-qPCR

Clinicopathological feature		N	Relevant expression of miR-452 (log2x)		
			Mean ± SD	T	P-value
Tissue	LUSC	23	5.350 ± 2.420	-0.671 ^a	0.509
	Adjacent non-cancer lung tissues	23	5.783 ± 1.847		
Age (years)	< 60	15	4.791 ± 2.048	-1.567	0.132
	≥ 60	8	6.399 ± 2.846		
Gender	Female	5	5.660 ± 1.491	-0.317	0.754
	Male	18	5.264 ± 2.650		
Smoking	No	12	5.783 ± 2.358	0.893	0.382
	Yes	11	4.877 ± 2.510		
Tumor size	≤ 3 cm	7	5.656 ± 3.099	0.393	0.698
	> 3 cm	16	5.216 ± 2.165		
Vascular invasion	No	20	5.503 ± 2.220	0.776	0.447
	Yes	3	4.330 ± 3.977		
TNM stage	I-II	10	7.110 ± 1.845	3.941	0.001*
	III-IV	13	3.996 ± 1.903		
Lymph node metastasis	No	11	6.191 ± 2.658	1.657	0.112
	Yes	12	4.579 ± 1.984		
Grade	II	16	5.472 ± 2.533	0.358	0.724
	III	7	5.071 ± 2.305		

^aStudent's paired t test was used for comparison between LUSC and non-cancer tissues. Student's unpaired t test was performed to evaluate miR-163 expression in different groups of clinical variables. *P < 0.05 was considered statistically significant.

35]. Gene Expression Profiling Interactive Analysis (GEPIA) (<http://gepia.cancer-pku.cn/>) is a web-based tool set up to allow exploration of TCGA and GTEx-derived cancer genomics data [36]. In this study, immunohistochemical results and box plots were downloaded from HPA, oncomine and GEPIA for the comparison of MTDH expression between LUSC and normal tissues.

Dual luciferase reporter assay

PsiCHECK-MTDH and psiCHECK-MTDH-mut 3'UTRs were constructed by DNA sequencing. HEK-293 T cells (5×10^4 per well) were grown in 24-well plates to reach a cell density of 70-80%. The cells were co-transfected with 50 nM miR-136-5p mimic (GenePharma, Shanghai, China), miR mimic control and 0.5 μ g reporter vector of psiCHECK-MTDH1 3'UTRs or psiCHECK-MTDH-1mut 3'UTRs. After 48 h of incubation, the ratios between renilla and firefly luciferase activity were estimated by Dual Luciferase Assay (Promega) according to the manufacturer's protocol. All the experiments were performed in triplicate.

Enrichment analyses of miR-136-5p candidate target genes in LUSC

To further investigate the underlying molecular mechanism of miR-136-5p in LUSC, bioinformatics analysis was performed. Firstly, genes overexpressed in LUSC from the TCGA database were obtained from GEPIA. Genes potentially targeted by miR-136-5p in LUSC were provided by 12 web-based prediction platforms (miRWalk, miRDB, PITA, RNAhybrid, miRNome, miRanda, PICTAR2, miRBridge, Targetscan, RNA22, MicroT4 and miRMap) and those predicted by no less than 5 platforms were further screened out. The overlap of genes was collected for subsequent enrichment analyses annotating Gene Ontology (GO) biological processes, cellular components and molecular functions combined with Kyoto Encyclopedia Genes and Genomes (KEGG) pathway terms. The entire enrichment analyses were carried out utilizing Metascape (<http://metascape.org>), a website designed to facilitate biomedicine research via comprehensive bioinformatics analysis [37].

MiR-136-5p and MTDH in lung squamous cell carcinoma

Table 3. Relationship between MTDH expression and clinico-pathological variables

Variables	Total (n)	MTDH expression n (%)		X ²	P
		Negative	Positive		
Tissue				6.037	0.014
LUSC	175	92 (52.6%)	83 (47.4%)		
Non-cancer tissues	30	23 (76.6%)	7 (23.3%)		
Gender				2.986	0.084
Male	172	101 (58.7%)	71 (41.3%)		
Female	33	14 (42.4%)	19 (57.6%)		
Age				1.965	0.161
< 60	107	65 (60.7%)	42 (39.3%)		
≥ 60	98	50 (51.0%)	48 (49.0%)		
Distant metastasis					0.709
No	168	89 (53.0%)	79 (47.0%)		
Yes	7	3 (42.9%)	4 (57.1%)		
Lymph node metastasis				6.621	0.010
No	118	70 (59.3%)	48 (40.7%)		
Yes	57	22 (38.6%)	35 (61.4%)		
TNM stage				1.792	0.181
I-II	148	81 (54.7%)	67 (45.3%)		
III-IV	27	11 (40.7%)	16 (59.3%)		
Tumor size				6.884	0.009
≤ 7 cm	155	87 (56.1%)	68 (43.9%)		
> 7 cm	20	5 (25.0%)	15 (75.0%)		
Tumor grade				1.639 ^a	0.441
I	31	14 (45.2%)	17 (54.8%)		
II	47	28 (59.6%)	19 (40.4%)		
III	97	50 (51.5%)	47 (48.5%)		

^aKruskal-Wallis H test was performed. The rest of the scores were from Chi-square test.

Statistical analysis

All the Statistical analyses for data from TCGA, RT-qPCR and IHC were performed on SPSS version 22.0. Expression values of miR-136-5p in LUSC and non-cancer tissues as well as the relative luciferase activity were presented in the form of mean (M) ± standard difference (SD). Student's paired t test was employed to assess the difference of miR-136-5p expression in LUSC and non-cancer tissues from RT-qPCR; while that from TCGA was calculated by Student's unpaired t test. The differential expression of miR-136-5p in various groups of clinico-pathological parameters and the statistical significance of relative luciferase activity in different groups were determined by independent sample's t test and one-way analysis of variance (ANOVA). The relationships between MTDH expression and the clinic-pathological parameters of LUSC were measured by Chi-

square test and Kruskal-Wallis H test. All *P*-values were 2-tailed, and *P* < 0.05 was set as the statistical significance level.

Results

Lower expression of miR-136-5p in LUSC from TCGA data

As illustrated in **Figure 1**, the expression of miR-136 was significantly down-regulated (6.701 ± 1.348) in LUSC compared with that in normal lung tissues (7.006 ± 0.898 , $t = -2.071$, $P = 0.042$, **Table 1** and **Figure 1**).

Lower miR-136-5p expression in LUSC tissues was significantly associated with TNM stage of LUSC

A total of 23 pairs of LUSC (15 cases age < 60, 8 cases age ≥ 60; 5 females, 18 males) and matched non-cancer lung tissues was detected

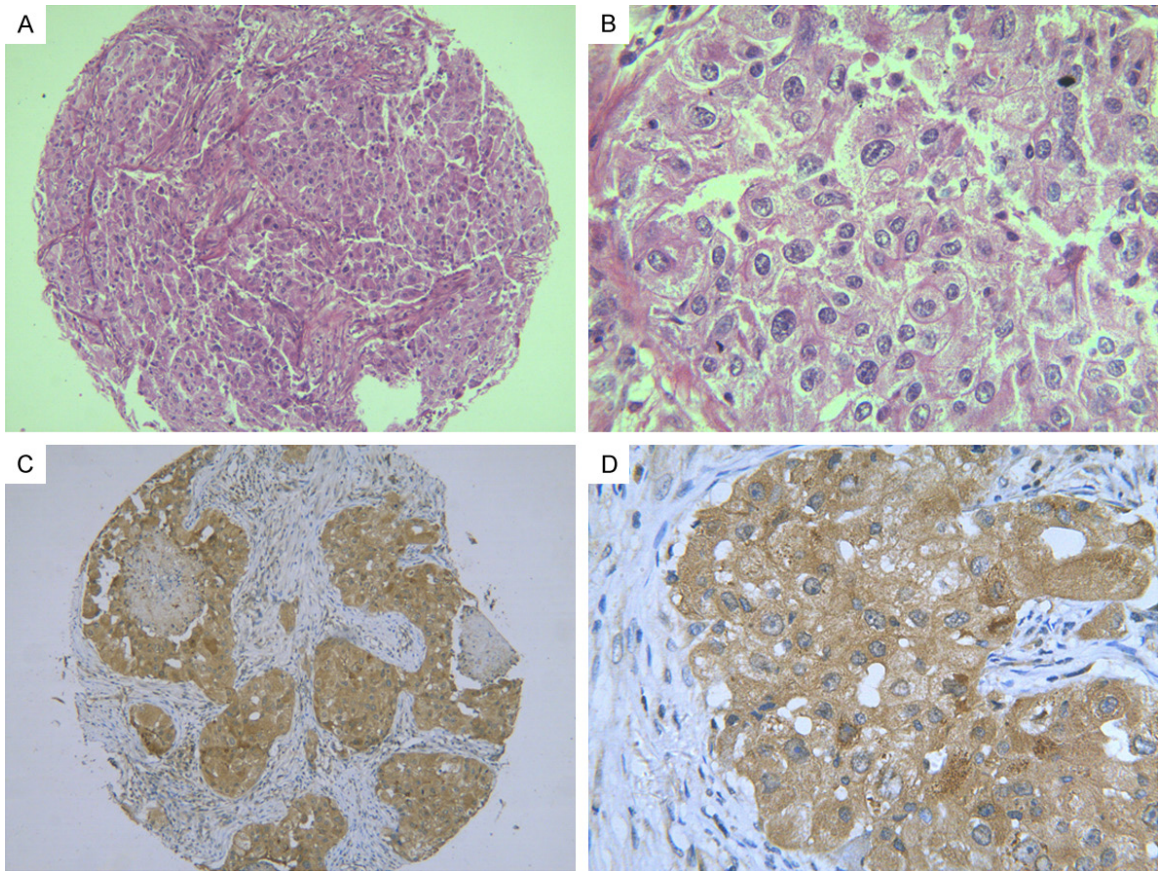


Figure 2. The representative staining pattern of MTDH in LUSC tissues and non-cancer tissues. Non-cancer lung tissues exhibited weak or no MTDH expression (A and B). MTDH expression was obviously observed in the cytoplasm of LUSC tissues (C and D). The magnification of (A and C) was 100 × and the magnification of (B and D) was 400 ×.

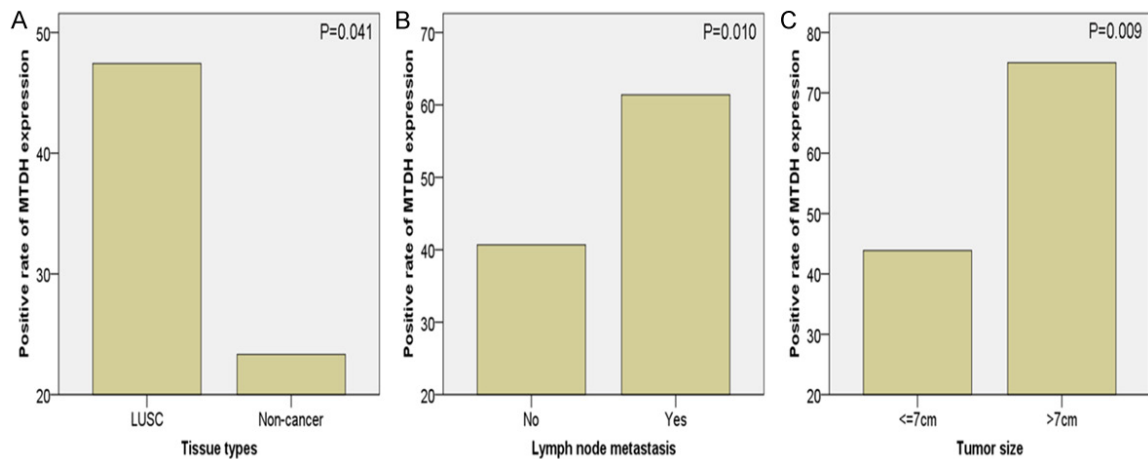


Figure 3. The relationship between MTDH expression and the clinicopathological variables of LUSC. A. The relationship between MTDH expression and tissue types. B. The relationship between MTDH expression and lymph node metastasis. C. The relationship between MTDH expression and tumor size. MTDH expression varied significantly in different subgroups of tissue types ($P = 0.041$), lymph node metastasis ($P = 0.010$) and tumor size ($P = 0.009$).

by RT-qPCR to assess the expression of miR-136-5p. The clinicopathological features of the

included samples were summarized in **Table 2**. There was a tendency of lower expression of

MiR-136-5p and MTDH in lung squamous cell carcinoma

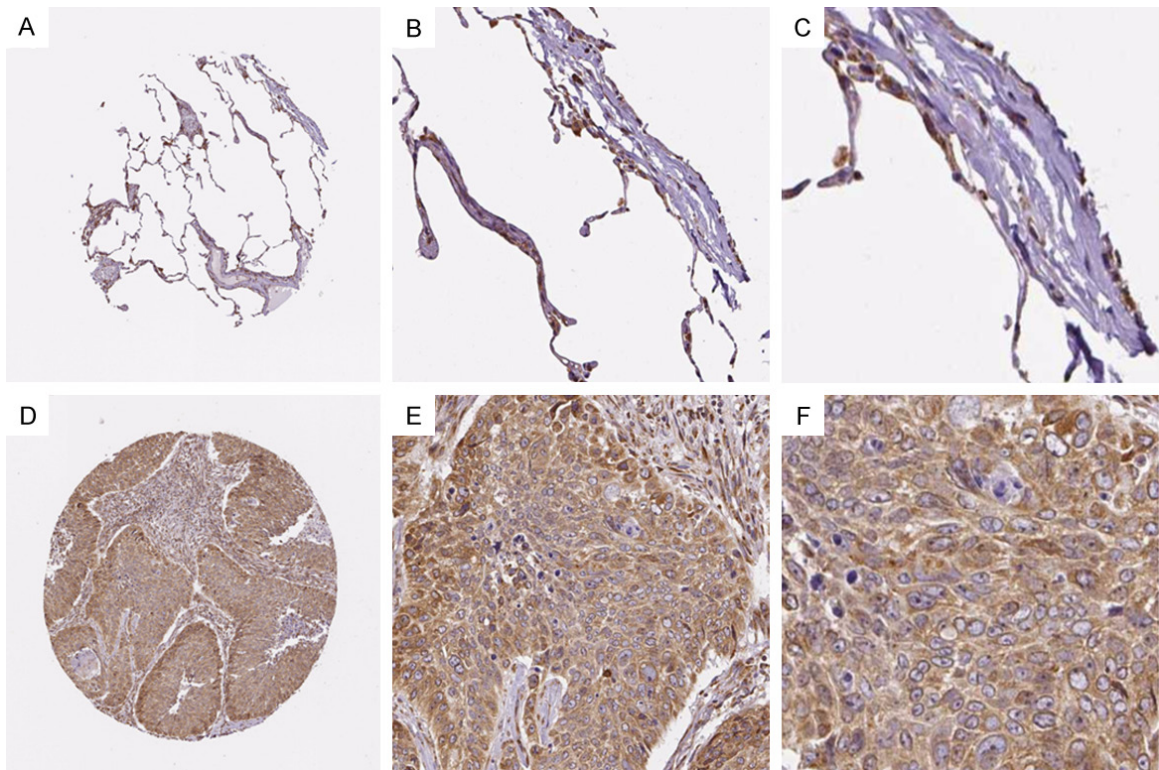
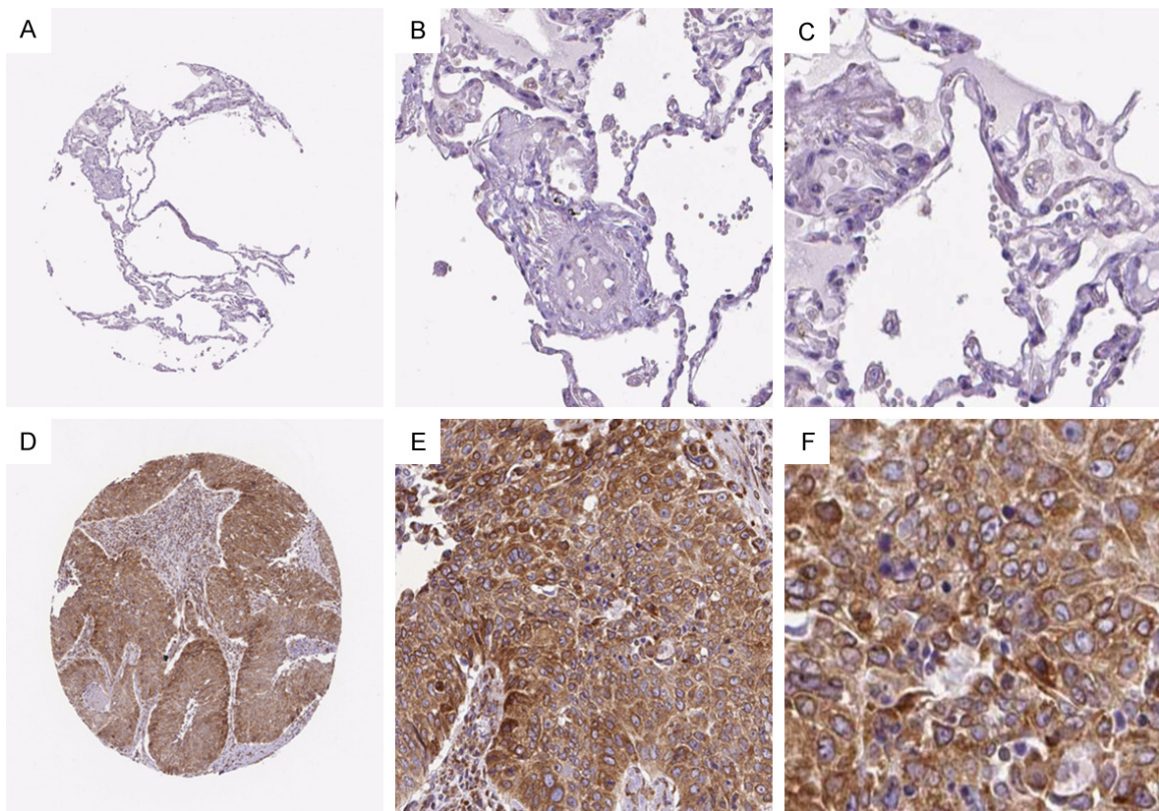


Figure 4. Immunostaining pattern of MTDH expression in LUSC and normal tissues using antibody HPA010932. A-C. No MTDH expression was detected in the pneumocytes of normal lung tissues. D-F. Moderate staining of MTDH in the cytoplasm of LUSC cells. All the immunostaining pictures were downloaded from HPA database.



MiR-136-5p and MTDH in lung squamous cell carcinoma

Figure 5. Immunostaining pattern of MTDH expression in LUSC and normal tissues using antibody CAB068204. A-C. No MTDH expression was detected in the pneumocytes of normal lung tissues. D-F. Moderate staining of MTDH in the cytoplasm of LUSC cells. All the immunostaining pictures were downloaded from HPA database.

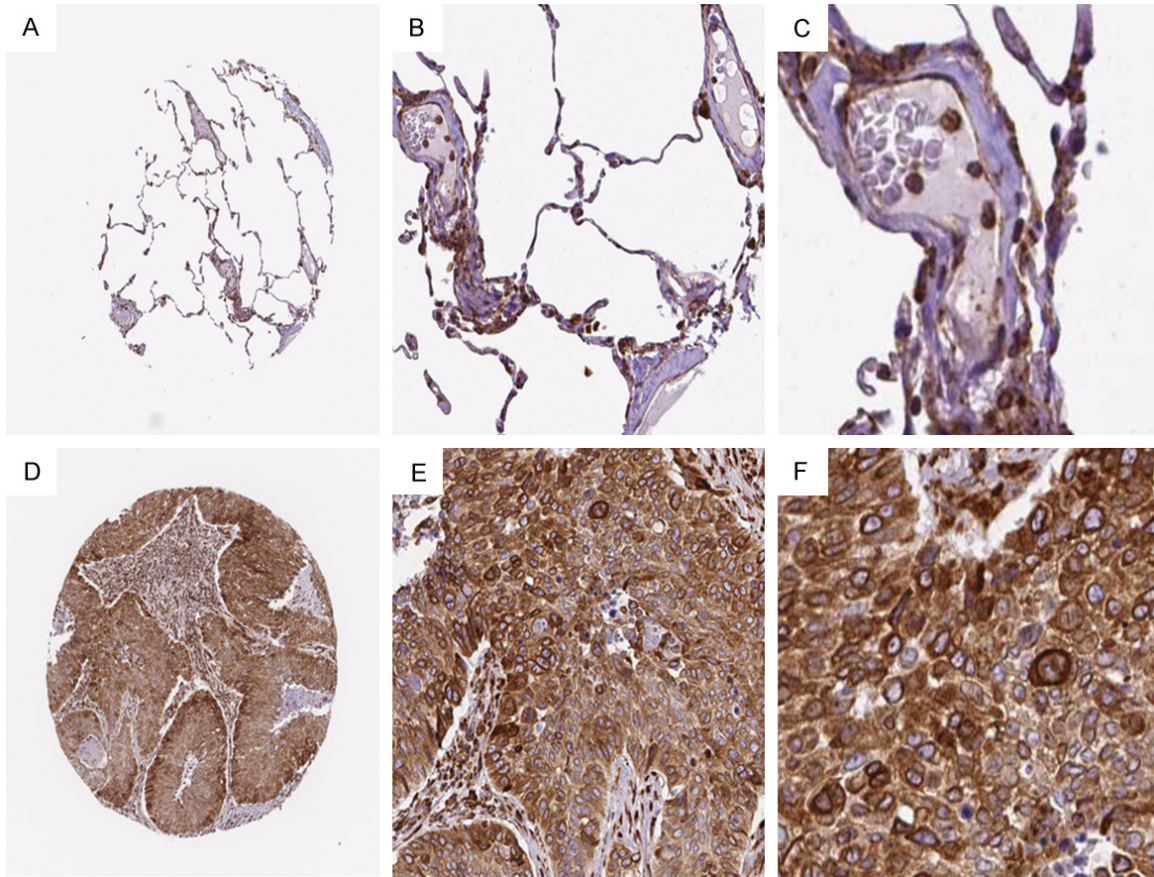


Figure 6. Immunostaining pattern of MTDH expression in LUSC and normal tissues using antibody CAB068205. A-C. No MTDH expression was detected in the pneumocytes of normal lung tissues. D-F. Strong staining of MTDH in the cytoplasm of LUSC cells. All the immunostaining pictures were downloaded from HPA database.

miR-136-5p (5.350 ± 2.420) in LUSC tissues than that in adjacent non-cancer lung tissues (5.783 ± 1.847 ; $P = 0.590$). Expression of miR-136-5p was significantly down-regulated in patients in advanced TNM stage (3.996 ± 1.903), compared with patients in early TNM stage (7.110 ± 1.845 ; $P = 0.001$). No significant relationships were found between miR136 expression and other clinic-pathological parameters of LUSC including age, gender, smoking status, tumor size, vascular invasion and lymph node metastasis and tumor grade.

IHC revealed significantly higher MTDH expression was significantly related to lymph node metastasis and tumor size in LUSC

The clinico-pathological information of the 175 LUSC patients and 30 non-cancer patients were listed in **Table 3**. Results from immuno-

taining showed that the positive rate of MTDH expression in 175 LUSC tissues (47.4%) was significantly higher than that in 30 non-cancer tissues (23.3%, $P = 0.041$) (**Figures 2, 3A**). MTDH also exhibited significantly higher expression in patients with lymph node metastasis (61.4%) than in patients without lymph node metastasis (40.7%, $P = 0.010$) (**Figure 3B**). In addition, a significantly higher expression of MTDH in patients with a tumor size of > 7 cm (75.0%) was observed, compared with that in patients with tumor size ≤ 7 cm (43.9%, $P = 0.009$) (**Figure 3C**).

Overexpression of MTDH in LUSC verified by multiple databases

IHC results from the HPA database indicated that MTDH was overexpressed in LUSC tissues, contrasting with the expression of MTDH in nor-

MiR-136-5p and MTDH in lung squamous cell carcinoma

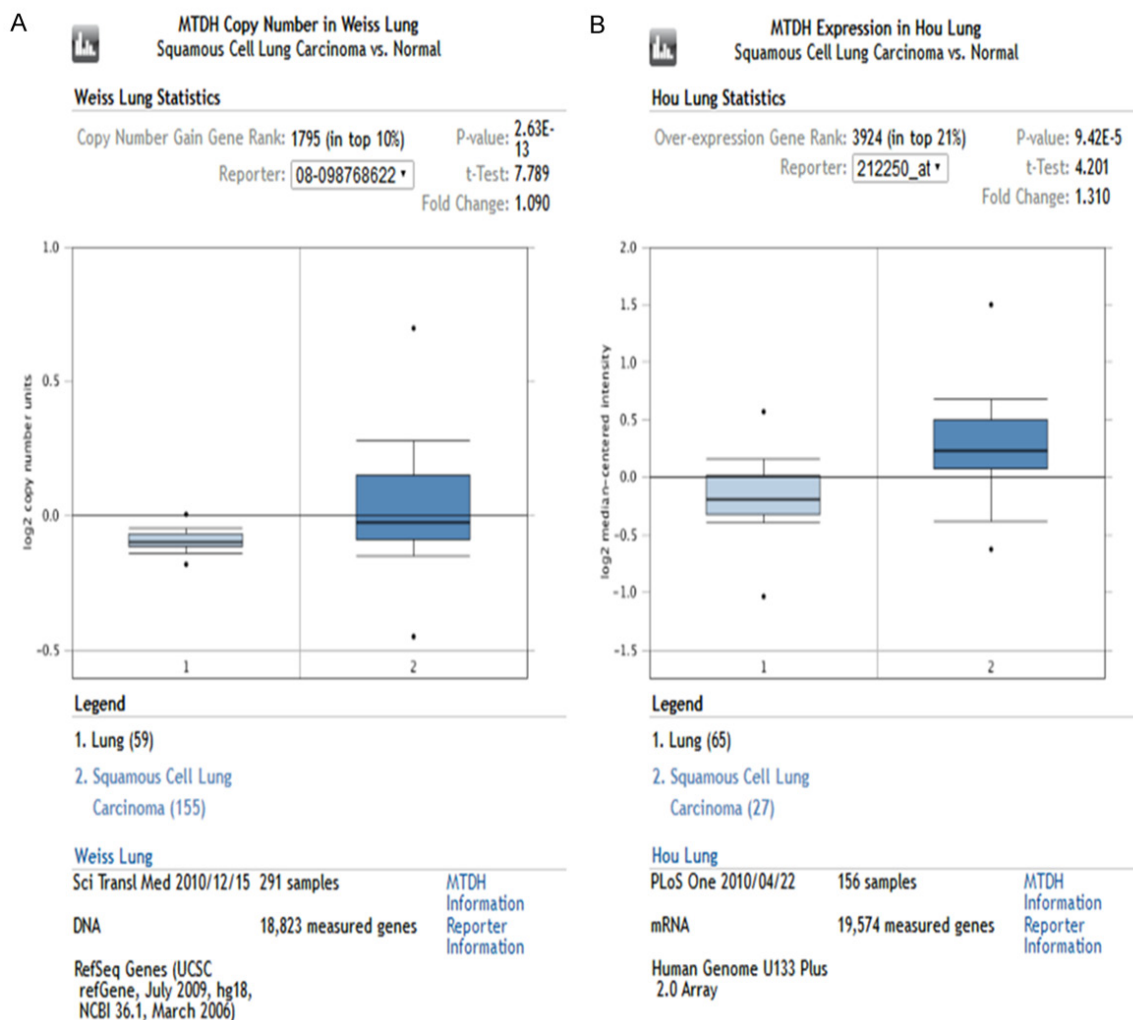


Figure 7. The difference of MTDH expression in LUSC and non-cancer tissues from Oncomine database. A. MTDH expression in 59 non-cancer lung tissues and 155 LUSC tissues from Weiss Lung Statistics ($P = 2.63 \times 10^{-13}$). B. MTDH expression in 65 non-cancer lung tissues and 27 LUSC tissues from Hou Lung Statistics ($P = 9.42 \times 10^{-5}$). MTDH expression was significantly higher in LUSC tissues than in normal tissues (Both $P < 0.05$).

mal tissues. Compared with the high (CAB068205) or moderate (CAB068204 and HPA010932) expression of MTDH in LUSC tissues, no expression of MTDH was observed in normal lung tissues (Figures 4-6). Positive staining of MTDH in LUSC presented diffuse or intense staining in the cytoplasm of LUSC cells, while no immunoreactivity of MTDH in pneumocytes of normal lung tissues was detected. Details of IHC staining in LUSC and normal tissues with different antibodies were illustrated in images at $\times 4$, $\times 40$, and $\times 100$ magnifications (Figures 5-7). The expression of MTDH in LUSC was also identified from two sets of data in the Oncomine database. Data from all sources consistently reflected the obviously higher

expression of MTDH in LUSC tissues than in non-cancer tissues ($P < 0.05$) (Figure 7). Additionally, Boxplot showing the expression of MTDH in 486 LUSC tissues and 338 normal tissues downloaded from GEPIA database revealed the same trend of overexpression of MTDH in LUSC tissues (Figure 8).

Targeting regulatory relationship between miR-136-5p and MTDH verified by dual luciferase reporter assay

We identified a binding site for miR-136-5p in the 3'-UTR of MTDH mRNA (Figure 9A). A luciferase reporter assay in HEK-293 T cells verifying the targeting regulatory relationship

MiR-136-5p and MTDH in lung squamous cell carcinoma

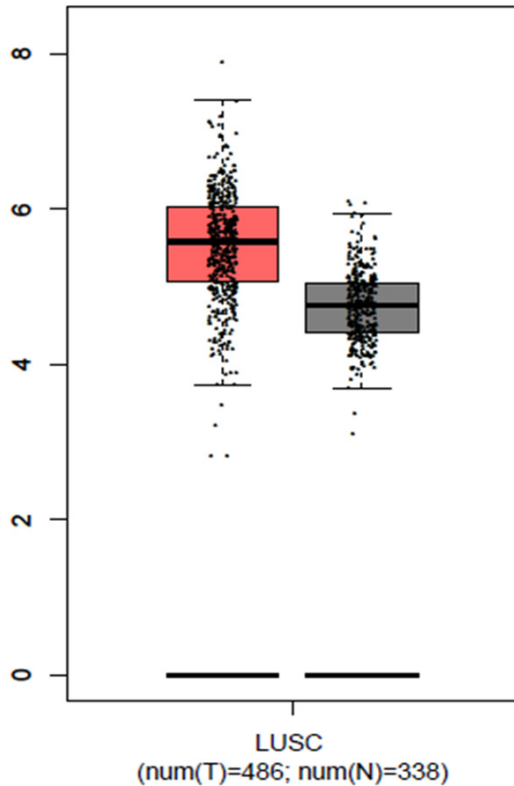


Figure 8. Expression of MTDH in LUSC and normal tissues from GEPIA. MTDH expression were detected in 486 LUSC tissues (T) and 338 normal tissues (N) from GEPIA. MTDH was overexpressed in BC tissues than in normal tissues. Axis units are Log₂ (TPM+1).

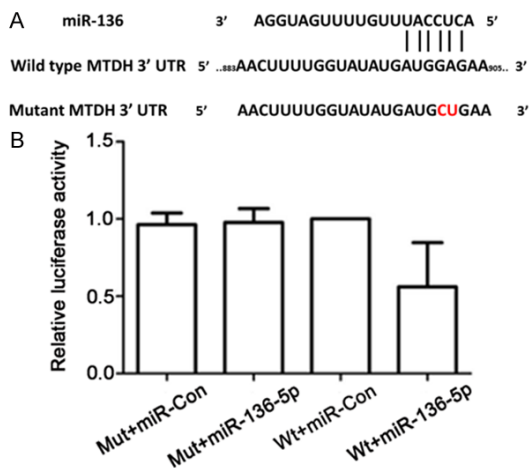


Figure 9. Dual luciferase reporter assay. A. The binding site for miR-136-5p in the 3'-UTR of MTDH mRNA. B. Luciferase activity of HEK-293T cells remarkably decreased after co-transfection with psiCHECK-2/MTDH 3'-UTR and miR-136-5p mimics.

between miR136 and MTDH was subsequently conducted. We found that the luciferase activi-

ty substantially decreased in HEK-293T cells co-transfected with psiCHECK-2/MTDH 3'-UTR and miR-136-5p-5p mimics, compared with controls (**Figure 9B**). This outcome revealed that MTDH was a direct target.

Enrichment analyses of candidate target genes

5964 overexpressed genes in LUSC from the TCGA database were identified while 3042 potential target genes of miR-136-5p in LUSC overlapped in no less than 5 online prediction programs. A total of 468 genes were perceived as candidate target genes of miR-136-5p in LUSC. These genes were uploaded to Metascape for enrichment analyses. GO terms pertinent to specific biological behaviors were aggregated amongst the candidate target genes with significant *P* value (all *P* < 0.01). For biological processes, vasculature development, small GTPase mediated signal transduction, muscle system process, regulation of cellular response to growth factor stimulus and transmembrane receptor protein tyrosine kinase signaling pathway were where the target genes mainly enriched. Regarding cellular components, leading edge membrane, plasma membrane protein complex, neuron projection membrane, cytoplasmic vesicle membrane and cell surface were of note. As for molecular function, target genes were mainly aggregated in guanyl-nucleotide exchange factor activity, proximal promoter sequence-specific DNA binding, complement component C3b binding, actin binding and phosphorus-oxygen lyase activity. Specific KEGG pathways were revealed, among which focal adhesion, MAPK signaling pathway and cytokine-cytokine receptor interaction are worthy of attention as they are well-known cancer-related pathways. Top terms of each category and relevant information were presented in **Table 4** and illustrated as heatmaps in **Figure 10**.

Discussion

To the best of our knowledge, there have been no efficacious therapeutic agents for the treatment of LUSC and the molecular mechanism responsible for the occurrence and development of LUSC was far from elucidated [38, 39]. Recently, an increasing body of evidence suggested that miRNAs were aberrantly expressed in LUSC and participated in the pathogenesis of LUSC by influencing the biological events of

MiR-136-5p and MTDH in lung squamous cell carcinoma

Table 4. Information of terms provided by enrichment analyses

ID	Category	Description	LogP	%InGO
GO:0001944	GO Biological Processes	Vasculature development	-13.76539383	11.13490364
GO:0001568	GO Biological Processes	Blood vessel development	-13.75691756	10.92077088
GO:0072358	GO Biological Processes	Cardiovascular system development	-13.57995077	11.13490364
GO:0048514	GO Biological Processes	Blood vessel morphogenesis	-12.61547361	9.850107066
GO:0001525	GO Biological Processes	Angiogenesis	-10.55279457	8.35117773
GO:0031256	GO Cellular Components	Leading edge membrane	-7.7685	3.640257
GO:0031252	GO Cellular Components	Cell leading edge	-6.55208	5.353319
GO:0031253	GO Cellular Components	Cell projection membrane	-4.45098	4.068522
GO:0001726	GO Cellular Components	Ruffle	-2.6416	2.141328
GO:0032587	GO Cellular Components	Ruffle membrane	-2.57343	1.498929
GO:0005085	GO Molecular Functions	Guanyl-nucleotide exchange factor activity	-7.14409	5.139186
GO:0051020	GO Molecular Functions	GTPase binding	-6.84211	7.494647
GO:0017016	GO Molecular Functions	Ras GTPase binding	-5.82891	6.20985
GO:0031267	GO Molecular Functions	Small GTPase binding	-5.55204	6.20985
GO:0005088	GO Molecular Functions	Ras guanyl-nucleotide exchange factor activity	-5.30279	3.85439
hsa05414	KEGG Pathway	Dilated cardiomyopathy	-6.46201	2.569593
hsa04261	KEGG Pathway	Adrenergic signaling in cardiomyocytes	-5.72725	2.997859
hsa05410	KEGG Pathway	Hypertrophic cardiomyopathy (HCM)	-4.25864	1.927195
hsa05412	KEGG Pathway	Arrhythmogenic right ventricular cardiomyopathy (ARVC)	-2.42272	1.284797
hsa04260	KEGG Pathway	Cardiac muscle contraction	-2.25171	1.284796574

LUSC [40-43]. Kumamoto T et al. reported that the significantly down-regulated miR-218 could induce the overexpression of TPD52, thereby enhance the migratory and invasive ability of LUSC cells [40]. A study by Qian L et al. revealed that miR-558 was remarkably down-regulated in LUSC tissues and miR-558 may inhibit the migration and invasion of LUSC cells via regulating GRN [44]. Similarly, members of the miR-29 family also played as a tumor suppressor in LUSC and reduced expression of miR-29 family strengthened cancer cell migration and invasion through directly mediating LOXL2 in LUSC. However, no documented association between miR-136-5p and LUSC was available in literature.

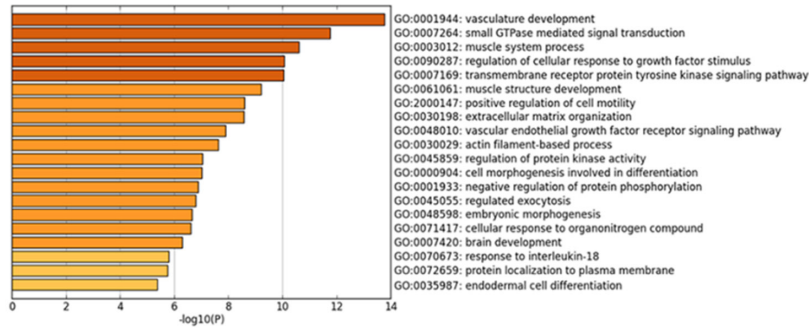
In the present study, we firstly examined the expression of miR-136-5p as well as the relationship between miR-136-5p expression and some clinico-pathological features of LUSC through TCGA. The results proved that miR-136-5p exhibited significantly lower expressed in LUSC than in non-cancer tissues. Data from RT-qPCR also revealed a tendency of lower expression of miR-136-5p in LUSC though with no statistical significance. We believe the result that miR-136-5p presented significant down-regulation in LUSC was convincing because the sample size of TCGA data was large (478

LUSC cases; 45 non-cancer cases). Moreover, a significant reverse correlation was observed between miR-136-5p expression and the TNM stages of LUSC from the RT-qPCR result, which hinted at the suppressive effect of miR-136-5p on the tumor progression of LUSC. We assumed that miR-136-5p might exert a tumor-suppressive function in LUSC.

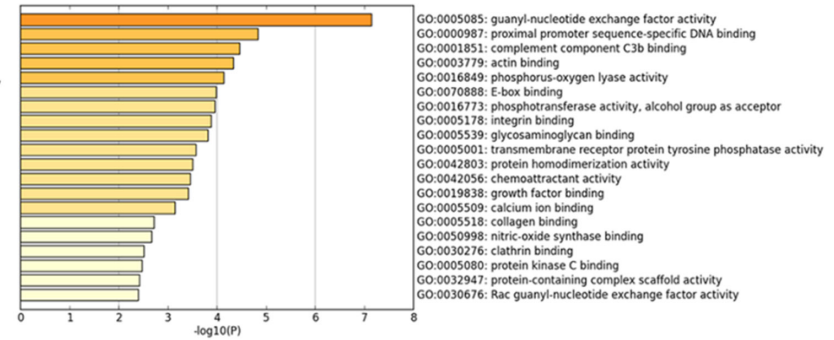
We went further to investigate the mechanism by which miR-136-5p was involved in the progression of LUSC. Since the biological functions of miRNAs were achieved by targeting the downstream molecules, focusing on the targets of miR-136-5p may facilitate our understanding of the miR-136-5p-related oncogenesis of LUSC. In this study, we concentrated on the targeting regulatory relationship between miR-136-5p and MTDH. Multiple approaches including IHC and data mining of public databases were utilized to evaluate the expression level of MTDH in LUSC. According to the results, data from IHC and public databases all supported the overexpression of MTDH in LUSC. Furthermore, the overexpression of MTDH was shown to be positively correlated with the malignant progression of LUSC, which implied that MTDH played the role of an oncogene in LUSC. Additionally, luciferase reporter assay provided evidence that MTDH was directly targeted by

MiR-136-5p and MTDH in lung squamous cell carcinoma

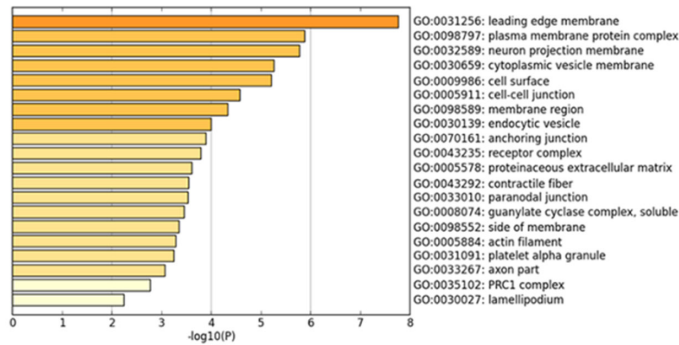
GO biological processes



GO molecular functions



GO cellular components



KEGG pathway

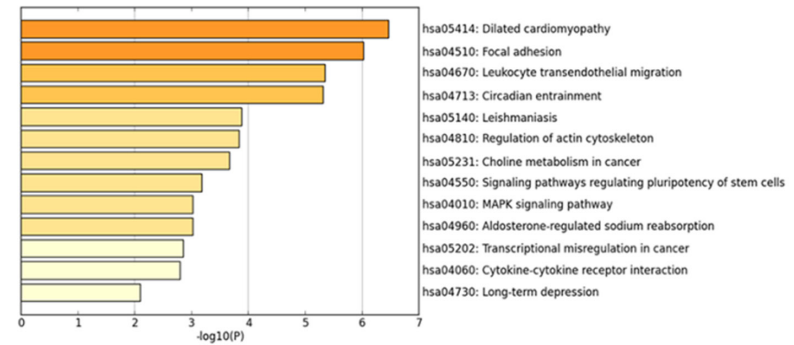


Figure 10. Heatmap of GO and KEGG enrichment analyses results.

miR-136-5p. Based on these findings, we conjectured that down-regulated miR-136-5p might contribute to the formation and development of LUSC through up-regulation of MTDH.

MTDH has been reported to be overexpressed in various human cancers such as hepatocellular carcinoma (HCC), gastric cancer, colorectal cancer and gallbladder carcinoma [45-47]. The effect of MTDH on tumor biology was multifaceted, which is embodied in the involvement of MTDH in the proliferation, invasion, chemoresistance, angiogenesis, and metastasis of cancer cells [46, 48-50]. The oncogenic function of MTDH on cancers can be explained by MTDH-induced activation of multiple pathways including phosphoinositide-3 kinase (PI3K)-Akt, mitogen-activated protein kinases (MAPKs), Wnt, and NF- κ B pathways [47, 51-53]. It is conceivable that MTDH might augment the malignant potential of LUSC via similar molecular machinery.

To further explore the molecular mechanism, we performed extra enrichment analyses comprising GO and KEGG pathway regarding the potential downstream target genes of miR-136-5p in LUSC. The results showed potential target genes of miR-136-5p were significantly enriched in the biological process vasculature development, implying that miR-136-5p might participate in tumor infiltration, angiogenesis and metastasis in LUSC. In regard to the KEGG pathway analysis, MAPK, an oncogenic pathway that can be activated by MTDH [51], was revealed to be involved in the pathogenesis of LUSC. The MAPKs regulate a wide range of cellular activities involved in tumor initiation progression. Specifically, extracellular signal-regulated kinase (ERK) is a main subgroup implicated in carcinogenesis [54-56]. Ying and colleagues [51] reported a significantly upregulation of MTDH expression in human retinoblastoma (RB) and suggested MTDH might be critical factors to trigger the MAPK pathway, resulting in fortified cancerous cell viability on account of their finding that knockdown of MTDH promoted the Bax/Bcl-2 ratio and caspase-3 in culture RB cells, modulated via the ERK signaling pathway. In LUSC, downregulated miR-136-5p might promote the expression of MTDH to affect tumor invasion, angiogenesis and metastasis, potentially via a similar pattern manipulated by the MAPK pathway. However,

further investigation is required to test the hypothesis.

In conclusion, miR-136-5p may serve as a tumor inhibitor in LUSC by targeting MTDH and miR-136-5p promises to be a candidate biomarker and therapeutic target for treating LUSC.

Disclosure of conflict of interest

None.

Address correspondence to: Weijia Mo, Department of Pathology, First Affiliated Hospital of Guangxi Medical University, Shuangyong Road, No. 6, Nanning, Guangxi Zhuang Autonomous Region, China. Tel: (+86) 15277192143; E-mail: gxmumo-weijia@163.com; Xiaojv Chi, Department of Medical Oncology, First Affiliated Hospital of Guangxi Medical University, Shuangyong Road, No. 6, Nanning, Guangxi Zhuang Autonomous Region, China. Tel: (+86) 0771-5356701; E-mail: 258043050@qq.com

References

- [1] Zhang Y, Li ZY, Hou XX, Wang X, Luo YH, Ying YP and Chen G. Clinical significance and effect of AEG-1 on the proliferation, invasion, and migration of NSCLC: a study based on immunohistochemistry, TCGA, bioinformatics, in vitro and in vivo verification. *Oncotarget* 2017; 8: 16531-16552.
- [2] Siegel RL, Miller KD and Jemal A. Cancer statistics, 2017. *CA Cancer J Clin* 2017; 67: 7-30.
- [3] Cao Y, Zhao D, Li P, Wang L, Qiao B, Qin X, Li L and Wang Y. MicroRNA-181a-5p impedes IL-17-induced nonsmall cell lung cancer proliferation and migration through targeting VCAM-1. *Cell Physiol Biochem* 2017; 42: 346-356.
- [4] Liu YZ, Yang H, Cao J, Jiang YY, Hao JJ, Xu X, Cai Y and Wang MR. KIAA1522 is a novel prognostic biomarker in patients with non-small cell lung cancer. *Sci Rep* 2016; 6: 24786.
- [5] Chen WJ, Gan TQ, Qin H, Huang SN, Yang LH, Fang YY, Li ZY, Pan LJ and Chen G. Implication of downregulation and prospective pathway signaling of microRNA-375 in lung squamous cell carcinoma. *Pathol Res Pract* 2017; 213: 364-372.
- [6] Zhang SY, Hui LP, Li CY, Gao J, Cui ZS and Qiu XS. More expression of BDNF associates with lung squamous cell carcinoma and is critical to the proliferation and invasion of lung cancer cells. *BMC Cancer* 2016; 16: 171.
- [7] Dolly SO, Collins DC, Sundar R, Popat S and Yap TA. Advances in the development of mo-

MiR-136-5p and MTDH in lung squamous cell carcinoma

- lecularly targeted agents in non-small-cell lung cancer. *Drugs* 2017; 77: 813-827.
- [8] Wilson FH, Johannessen CM, Piccioni F, Tamayo P, Kim JW, Van Allen EM, Corsello SM, Capelletti M, Calles A, Butaney M, Sharifnia T, Gabriel SB, Mesirov JP, Hahn WC, Engelman JA, Meyerson M, Root DE, Janne PA and Garraway LA. A functional landscape of resistance to ALK inhibition in lung cancer. *Cancer Cell* 2015; 27: 397-408.
- [9] Zhang N, Zeng Y, Du W, Zhu J, Shen D, Liu Z and Huang JA. The EGFR pathway is involved in the regulation of PD-L1 expression via the IL-6/JAK/STAT3 signaling pathway in EGFR-mutated non-small cell lung cancer. *Int J Oncol* 2016; 49: 1360-1368.
- [10] Politi K, Ayeni D and Lynch T. The next wave of EGFR tyrosine kinase inhibitors enter the clinic. *Cancer Cell* 2015; 27: 751-753.
- [11] Liu C, Xu X and Zhou Y. Association between EGFR polymorphisms and the risk of lung cancer. *Int J Clin Exp Pathol* 2015; 8: 15245-15249.
- [12] Bashirullah A, Pasquinelli AE, Kiger AA, Perrimon N, Ruvkun G and Thummel CS. Coordinate regulation of small temporal RNAs at the onset of *Drosophila* metamorphosis. *Dev Biol* 2003; 259: 1-8.
- [13] Palma Flores C, Garcia-Vazquez R, Gallardo Rincon D, Ruiz-Garcia E, Astudillo de la Vega H, Marchat LA, Salinas Vera YM and Lopez-Camarillo C. MicroRNAs driving invasion and metastasis in ovarian cancer: opportunities for translational medicine (Review). *Int J Oncol* 2017; 50: 1461-1476.
- [14] Wu C, Zhuang Y, Jiang S, Liu S, Zhou J, Wu J, Teng Y, Xia B, Wang R and Zou X. Interaction between Wnt/beta-catenin pathway and microRNAs regulates epithelial-mesenchymal transition in gastric cancer (Review). *Int J Oncol* 2016; 48: 2236-2246.
- [15] He RQ, Li XJ, Liang L, Xie Y, Luo DZ, Ma J, Peng ZG, Hu XH and Chen G. The suppressive role of miR-542-5p in NSCLC: the evidence from clinical data and in vivo validation using a chick chorioallantoic membrane model. *BMC Cancer* 2017; 17: 655.
- [16] Tang RX, Chen WJ, He RQ, Zeng JH, Liang L, Li SK, Ma J, Luo DZ and Chen G. Identification of a RNA-Seq based prognostic signature with five lncRNAs for lung squamous cell carcinoma. *Oncotarget* 2017; 8: 50761-50773.
- [17] Li Z, Yu X, Shen J, Law PT, Chan MT and Wu WK. MicroRNA expression and its implications for diagnosis and therapy of gallbladder cancer. *Oncotarget* 2015; 6: 13914-13921.
- [18] Yu X and Li Z. The role of microRNAs expression in laryngeal cancer. *Oncotarget* 2015; 6: 23297-23305.
- [19] Cekaite L, Eide PW, Lind GE, Skotheim RI and Lothe RA. MicroRNAs as growth regulators, their function and biomarker status in colorectal cancer. *Oncotarget* 2016; 7: 6476-6505.
- [20] Shen S, Yue H, Li Y, Qin J, Li K, Liu Y and Wang J. Upregulation of miR-136 in human non-small cell lung cancer cells promotes Erk1/2 activation by targeting PPP2R2A. *Tumour Biol* 2014; 35: 631-640.
- [21] Yang Y, Liu L, Cai J, Wu J, Guan H, Zhu X, Yuan J, Chen S and Li M. Targeting Smad2 and Smad3 by miR-136 suppresses metastasis-associated traits of lung adenocarcinoma cells. *Oncol Res* 2013; 21: 345-352.
- [22] Zhao J, Wang W, Huang Y, Wu J, Chen M, Cui P, Zhang W and Zhang Y. HBx elevates oncoprotein AEG-1 expression to promote cell migration by downregulating miR-375 and miR-136 in malignant hepatocytes. *DNA Cell Biol* 2014; 33: 715-722.
- [23] Zheng J, Ge P, Liu X, Wei J, Wu G and Li X. MiR-136 inhibits gastric cancer-specific peritoneal metastasis by targeting HOXC10. *Tumour Biol* 2017; 39: 1010428317706207.
- [24] Jeong JY, Kang H, Kim TH, Kim G, Heo JH, Kwon AY, Kim S, Jung SG and An HJ. MicroRNA-136 inhibits cancer stem cell activity and enhances the anti-tumor effect of paclitaxel against chemoresistant ovarian cancer cells by targeting Notch3. *Cancer Lett* 2017; 386: 168-178.
- [25] Yan M, Li X, Tong D, Han C, Zhao R, He Y and Jin X. miR-136 suppresses tumor invasion and metastasis by targeting RASAL2 in triple-negative breast cancer. *Oncol Rep* 2016; 36: 65-71.
- [26] Wu H, Liu Q, Cai T, Chen YD, Liao F and Wang ZF. MiR-136 modulates glioma cell sensitivity to temozolomide by targeting astrocyte elevated gene-1. *Diagn Pathol* 2014; 9: 173.
- [27] Huang Y, Ren GP, Xu C, Dong SF, Wang Y, Gan Y, Zhu L and Feng TY. Expression of astrocyte elevated gene-1 (AEG-1) as a biomarker for aggressive pancreatic ductal adenocarcinoma. *BMC Cancer* 2014; 14: 479.
- [28] Mataka H, Seki N, Mizuno K, Nohata N, Kamikawaji K, Kumamoto T, Koshizuka K, Goto Y and Inoue H. Dual-strand tumor-suppressor microRNA-145 (miR-145-5p and miR-145-3p) coordinately targeted MTDH in lung squamous cell carcinoma. *Oncotarget* 2016; 7: 72084-72098.
- [29] Chen G, Kronenberger P, Teugels E, Umelo IA and De Greve J. Targeting the epidermal growth factor receptor in non-small cell lung cancer cells: the effect of combining RNA interference with tyrosine kinase inhibitors or cetuximab. *BMC Med* 2012; 10: 28.
- [30] Chen G, Umelo IA, Lv S, Teugels E, Fostier K, Kronenberger P, Dewaele A, Sadones J, Geers

- C and De Greve J. miR-146a inhibits cell growth, cell migration and induces apoptosis in non-small cell lung cancer cells. *PLoS One* 2013; 8: e60317.
- [31] Rong M, He R, Dang Y and Chen G. Expression and clinicopathological significance of miR-146a in hepatocellular carcinoma tissues. *Ups J Med Sci* 2014; 119: 19-24.
- [32] Chen G, Kronenberger P, Teugels E and De Greve J. Influence of RT-qPCR primer position on EGFR interference efficacy in lung cancer cells. *Biol Proced Online* 2010; 13: 1.
- [33] Thul PJ and Lindskog C. The human protein atlas - a spatial map of the human proteome. *Protein Sci* 2018; 27: 233-244.
- [34] Rhodes DR, Kalyana-Sundaram S, Mahavisno V, Varambally R, Yu J, Briggs BB, Barrette TR, Anstet MJ, Kincead-Beal C, Kulkarni P, Varambally S, Ghosh D and Chinnaiyan AM. Oncomine 3.0: genes, pathways, and networks in a collection of 18,000 cancer gene expression profiles. *Neoplasia* 2007; 9: 166-180.
- [35] Rhodes DR, Yu J, Shanker K, Deshpande N, Varambally R, Ghosh D, Barrette T, Pandey A and Chinnaiyan AM. ONCOMINE: a cancer microarray database and integrated data-mining platform. *Neoplasia* 2004; 6: 1-6.
- [36] Tang Z, Li C, Kang B, Gao G, Li C and Zhang Z. GEPIA: a web server for cancer and normal gene expression profiling and interactive analyses. *Nucleic Acids Res* 2017; 45: W98-W102.
- [37] Tripathi S, Pohl MO, Zhou Y, Rodriguez-Frandsen A, Wang G, Stein DA, Moulton HM, DeJesus P, Che J, Mulder LC, Yanguez E, Andenmatten D, Pache L, Manicassamy B, Albrecht RA, Gonzalez MG, Nguyen Q, Brass A, Elledge S, White M, Shapira S, Hacohen N, Karlas A, Meyer TF, Shales M, Gatorano A, Johnson JR, Jang G, Johnson T, Verschuere E, Sanders D, Krogan N, Shaw M, Konig R, Stertz S, Garcia-Sastre A and Chanda SK. Meta- and orthogonal integration of influenza "OMICs" data defines a role for UBR4 in virus budding. *Cell Host Microbe* 2015; 18: 723-735.
- [38] Li K, Pan X, Bi Y, Xu W, Chen C, Gao H, Shi B, Jiang H, Yang S, Jiang L and Li Z. Adoptive immunotherapy using T lymphocytes redirected to glypican-3 for the treatment of lung squamous cell carcinoma. *Oncotarget* 2016; 7: 2496-2507.
- [39] Li F, Han X, Li F, Wang R, Wang H, Gao Y, Wang X, Fang Z, Zhang W, Yao S, Tong X, Wang Y, Feng Y, Sun Y, Li Y, Wong KK, Zhai Q, Chen H and Ji H. LKB1 inactivation elicits a redox imbalance to modulate non-small cell lung cancer plasticity and therapeutic response. *Cancer Cell* 2015; 27: 698-711.
- [40] Kumamoto T, Seki N, Mataka H, Mizuno K, Kamikawaji K, Samukawa T, Koshizuka K, Goto Y and Inoue H. Regulation of TPD52 by antitumor microRNA-218 suppresses cancer cell migration and invasion in lung squamous cell carcinoma. *Int J Oncol* 2016; 49: 1870-1880.
- [41] Mizuno K, Seki N, Mataka H, Matsushita R, Kamikawaji K, Kumamoto T, Takagi K, Goto Y, Nishikawa R, Kato M, Enokida H, Nakagawa M and Inoue H. Tumor-suppressive microRNA-29 family inhibits cancer cell migration and invasion directly targeting LOXL2 in lung squamous cell carcinoma. *Int J Oncol* 2016; 48: 450-460.
- [42] Rapp J, Kiss E, Meggyes M, Szabo-Meleg E, Feller D, Smuk G, Laszlo T, Sarosi V, Molnar TF, Kvell K and Pongracz JE. Increased Wnt5a in squamous cell lung carcinoma inhibits endothelial cell motility. *BMC Cancer* 2016; 16: 915.
- [43] Gao X, Wang Y, Zhao H, Wei F, Zhang X, Su Y, Wang C, Li H and Ren X. Plasma miR-324-3p and miR-1285 as diagnostic and prognostic biomarkers for early stage lung squamous cell carcinoma. *Oncotarget* 2016; 7: 59664-59675.
- [44] Qian L, Lin L, Du Y, Hao X, Zhao Y and Liu X. MicroRNA-588 suppresses tumor cell migration and invasion by targeting GRN in lung squamous cell carcinoma. *Mol Med Rep* 2016; 14: 3021-3028.
- [45] He R, Gao L, Ma J, Peng Z, Zhou S, Yang L, Feng Z, Dang Y and Chen G. The essential role of MTDH in the progression of HCC: a study with immunohistochemistry, TCGA, meta-analysis and in vitro investigation. *Am J Transl Res* 2017; 9: 1561-1579.
- [46] Qiao W, Cao N and Yang L. MicroRNA-154 inhibits the growth and metastasis of gastric cancer cells by directly targeting MTDH. *Oncol Lett* 2017; 14: 3268-3274.
- [47] Huang Y and Li LP. Progress of cancer research on astrocyte elevated gene-1/metadherin (Review). *Oncol Lett* 2014; 8: 493-501.
- [48] Wang Y, Wei Y, Tong H, Chen L, Fan Y, Ji Y, Jia W, Liu D and Wang G. MiR-302c-3p suppresses invasion and proliferation of glioma cells via down-regulating metadherin (MTDH) expression. *Cancer Biol Ther* 2015; 16: 1308-1315.
- [49] Li PP, Feng LL, Chen N, Lu K, Meng XH, Ge XL, Lv X and Wang X. Metadherin interference inhibits proliferation and enhances chemosensitivity to doxorubicin in diffuse large B cell lymphoma. *Int J Clin Exp Med* 2014; 7: 2081-2086.
- [50] Liu Y, Kong X, Li X, Li B and Yang Q. Knockdown of metadherin inhibits angiogenesis in breast cancer. *Int J Oncol* 2015; 46: 2459-2466.
- [51] Chang Y, Li B, Xu X, Shen L, Bai H, Gao F, Zhang Z and Jonas JB. Lentivirus-mediated knockdown of astrocyte elevated gene-1 inhibits growth and induces apoptosis through mapk

MiR-136-5p and MTDH in lung squamous cell carcinoma

- pathways in human retinoblastoma cells. *PLoS One* 2016; 11: e0148763.
- [52] Liang X, Li H, Fu D, Chong T, Wang Z and Li Z. MicroRNA-1297 inhibits prostate cancer cell proliferation and invasion by targeting the AEG-1/Wnt signaling pathway. *Biochem Biophys Res Commun* 2016; 480: 208-214.
- [53] Wang Z, Cao CJ, Huang LL, Ke ZF, Luo CJ, Lin ZW, Wang F, Zhang YQ and Wang LT. EFEMP1 promotes the migration and invasion of osteosarcoma via MMP-2 with induction by AEG-1 via NF-kappaB signaling pathway. *Oncotarget* 2015; 6: 14191-14208.
- [54] Rocca S, Carra G, Poggio P, Morotti A and Brancaccio M. Targeting few to help hundreds: JAK, MAPK and ROCK pathways as druggable targets in atypical chronic myeloid leukemia. *Mol Cancer* 2018; 17: 40.
- [55] Dinsmore CJ and Soriano P. MAPK and PI3K signaling: at the crossroads of neural crest development. *Dev Biol* 2018; [Epub ahead of print].
- [56] Peluso I, Yarla NS, Ambra R, Pastore G and Perry G. MAPK signalling pathway in cancers: olive products as cancer preventive and therapeutic agents. *Semin Cancer Biol* 2017; [Epub ahead of print].